

Tantalum–Gold and Tantalum–Copper Trihydride Complexes $[\text{Cp}'_2\text{TaH}_3\text{MPPPh}_3][\text{PF}_6]$ ($\text{Cp}' = \text{C}_5\text{H}_4\text{C}(\text{CH}_3)_3$). Structure Determination from ^1H T_1 Relaxation Studies

Vladimir I. Bakhmutov,^{*,†} Evgenii V. Vorontsov,[†] Ekaterina V. Bakhmutova,[†] Gilles Boni,[‡] and Claude Moise^{*,‡}

Institute of Organo-Element Compounds, Russian Academy of Sciences, Vavilov Street 28, Moscow 117813, Russia, and Laboratoire de synthese et electrosynthese organometalliques, UMR 5632, CNRS, 6 Bd Gabriel, F-21000, Dijon, France

Received July 7, 1998

The reaction of $\text{Cp}'_2\text{TaH}_3$ ($\text{Cp}' = \text{C}_5\text{H}_4\text{C}(\text{CH}_3)_3$) with $[\text{MPPPh}_3][\text{PF}_6]$ yields the bimetallic complexes $[\text{Cp}'_2\text{TaH}_3\text{-MPPPh}_3][\text{PF}_6]$ ($\text{M} = \text{Au}$ (**1**), $\text{M} = \text{Cu}$ (**2**)). The detailed NMR study of **1** and **2** showed the structure with two bridging hydride ligands. The mutual orientation of the Cp' rings has been determined by NOE experiments. The variable-temperature NMR data showed an intramolecular exchange between two outer hydride ligands. The exchange is faster in **1** ($\Delta G^\ddagger(210\text{ K}) = 9.3\text{ kcal/mol}$) than in **2** ($\Delta H^\ddagger = 8.6 \pm 0.2\text{ kcal/mol}$, $\Delta S^\ddagger = -5.0 \pm 0.4\text{ eu}$, $\Delta G^\ddagger(210\text{ K}) = 9.6 \pm 0.2\text{ kcal/mol}$). In contrast, complex **2** undergoes the faster intermolecular $\text{PPh}_3/\text{PPh}_3$ exchange. It has been demonstrated that $T_{1\text{min}}$, T_1 , $T_{1\text{sel}}$ and $T_{1\text{bis}}$ measurements are a powerful instrument for quantitative localization of the hydride ligands in solutions of bimetallic complexes. The determined hydride–hydride and metal–hydride distances reproduce well the structural tendencies in the related niobium trihydride $[\{\text{Nb}(\text{C}_5\text{H}_3\text{RR}')_2\text{H}_3\}_2\text{Au}][\text{PF}_6]$ ($\text{R} = \text{R}' = \text{Si}(\text{CH}_3)_3$) established by the X-ray method. Tantalum–gold complex **1** showed weak exchange couplings.

Introduction

Transition metal hydride complexes represent one of the most important classes of inorganic compounds due to their reactivity and importance in catalysis.¹ Among the hydride complexes, bimetallic polyhydrides are of special interest^{1b} because of the presence of terminal and bridging hydride ligands binding to different metal centers.

Since the discovery of ($\eta^2\text{-H}_2$) complexes,² the NMR spin–lattice (T_1) relaxation has attracted the significant attention of inorganic chemists as a reliable instrument for structural characterizations of transition metal hydrides in solution. The theoretical analysis and practical examples³ revealed that $T_{1\text{min}}$ measurements of classical *mononuclear* transition metal hydrides provide determination of the M-H and $\text{H}\cdots\text{H}$ distances in good agreement with the neutron diffraction method. In the present work, we demonstrate how the M-H and $\text{H}\cdots\text{H}$ distances can be deduced from measurements of nonselective (T_1), selective ($T_{1\text{sel}}$), and biselective ($T_{1\text{bis}}$) relaxation times of the hydride ligands in *bimetallic* hydride complexes. We report here the preparation of new mixed tantalum–gold and tantalum–copper trihydrides of the formula $[\text{Cp}'_2\text{TaH}_3\text{MPPPh}_3][\text{PF}_6]$ ($\text{M} = \text{Au}$ (**1**), Cu (**2**); $\text{Cp}' = \text{C}_5\text{H}_4\text{C}(\text{CH}_3)_3$) with two bridging hydride ligands. The structures of these compounds were established from relaxation measurements and by an analysis of the proton–

proton and phosphorus–proton coupling constants in the low-temperature NMR spectra. In addition, NOE experiments were carried out to support the suggested structures. Tantalum–gold complex **1** showed weak exchange couplings.

Experimental Section

The NMR studies were carried out in NMR tubes sealed under a dry Ar atmosphere. NMR data were collected with Bruker WP 200 SY and AMX 400 spectrometers. The conventional inversion–recovery method ($180^\circ - \tau - 90^\circ$) was used to determine T_1 . $T_{1\text{sel}}$ relaxation times were measured by applying a selective 180° pulse provided by the decoupler systems. The duration and the power of the selective pulses were regulated to excite only one of the hydride resonances. $T_{1\text{bis}}$ relaxation times were determined by applying selective 180° pulses exciting two resonance lines. The calculation of the relaxation times was made using the nonlinear three-parameter fitting routine of the spectrometers. In each relaxation experiment, the waiting period was 5 times larger than the expected relaxation time and 16–18 variable delays were employed. The durations of the pulses were controlled at every temperature. The errors in T_1 determinations were lower than 5% (this was checked with different samples). The rate constants for the hydride/hydride exchange in complex **2** (from 190 to 280 K the rate constant takes the values between 37.3 and $6.17 \times 10^4\text{ s}^{-1}$) were calculated from the variable-temperature ^1H NMR spectra using the program DNMR-5.

IR spectra were recorded as Nujol mulls between KBr or CaF_2 plates using a Specord M82 spectrometer. Compound **1**: 1708 (w), 1685 (w) ($\nu(\text{Ta-H})$); 838 (s, br) ($\nu(\text{PF}_6^-)$); 1610 (m), 1583 (m) ($\nu(\text{Ar})$); 749 (s), 696 (s) cm^{-1} ($\rho(\text{CH})_{\text{Ar}}$). Compound **2**: 1701 (vw), 1665 (vw) ($\nu(\text{Ta-H})$); 840 (s, br) ($\nu(\text{PF}_6^-)$); 1559 (m), 1584 (m) ($\nu(\text{Ar})$); 743 (s), 696 (s) cm^{-1} ($\rho(\text{CH})_{\text{Ar}}$).

Elemental analyses of **1** and **2** were performed on an EA 1108 CHNS-O FISONIS Instrument.

Preparation of $[\text{Cp}'_2\text{TaH}_3\text{MPPPh}_3][\text{PF}_6]$. All manipulations were performed under an argon atmosphere by standard techniques. Solvents were dried and degassed by using conventional procedures. The

[†] Russian Academy of Sciences.

[‡] CNRS.

- (1) (a) Hlatky, G. G.; Crabtree, R. H. *Coord. Chem. Rev.* **1985**, *65*, 1. (b) Venanzi, L. M. *Coord. Chem. Rev.* **1982**, *43*, 251.
- (2) Kubas, G. J. *Acc. Chem. Res.* **1988**, *21*, 120.
- (3) (a) Gusev, D. G.; Nietlispach, D.; Vymenits, A. B.; Bakhmutov, V. I.; Berke, H. *Inorg. Chem.* **1993**, *32*, 3270. (b) Bakhmutov, V. I.; Vorontsov, E. V.; Nikonov, G. I.; Lemenovskii, D. A. *Inorg. Chem.* **1998**, *37*, 279. (c) Bakhmutov, V. I.; Vorontsov, E. V. *Rev. Inorg. Chem.* **1998**, *18*, 183.

Table 1. Room-Temperature ^1H NMR Data for Complexes **1** and **2** in Acetone- d_6

proton	δ , ^a ppm	T_{min} , s (T , K) ^b	$J(\text{H}-\text{P})$, Hz	$J(\text{H}-\text{H})$, Hz
Complex 1				
H ^X	0.131	0.0962 (210)	21.0	2.8
H ^A	-0.714	0.0754 (210)	62.2	2.8
CH ₃	1.335	0.111 (205)		
Cp(H ^a)	5.369	0.398 (210)		2.2
Cp(H ^b)	5.881	0.506 (210)		2.2
Complex 2				
H ^X	-2.490	0.0934 (200)		7.8
H ^A	-3.629	0.0715 (200)		7.8
CH ₃	1.338	0.0954 (190–200)		
Cp(H ^a)	5.198	0.300 (190–200)		2.2
Cp(H ^b)	5.696	0.399 (190–200)		2.2

^a $\delta(\text{Ph}) = 7.65$ and 7.33 ppm for **1** and **2**, respectively. ^b At 200 MHz.

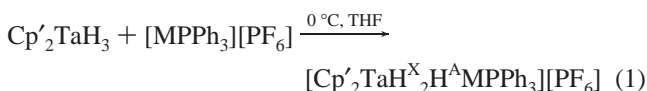
following compounds were prepared as described in the literature: $(\text{C}_5\text{H}_4\text{Bu}^t)_2\text{TaH}_3$,^{4a} CuPPh_3Cl ,^{4b} and AuPPh_3Cl .^{4c}

[(C₅H₄Bu^t)₂TaH₃Cu(PPh₃)] [PF₆]. A THF solution of $[\text{CuPPh}_3][\text{PF}_6]$ (0.40 mmol) prepared in situ from $[\text{CuPPh}_3\text{Cl}]_4$ (300 mg, 0.10 mmol) and TlPF₆ (150 mg, 0.40 mmol) (the TlCl precipitate was eliminated by filtration) was added to a THF solution (30 mL) of $(\text{C}_5\text{H}_4\text{Bu}^t)_2\text{TaH}_3$ (0.40 mmol) at 0 °C. The reaction mixture was stirred for 15 min to yield a colorless solution with a precipitate. The precipitate was filtered off, and the solvent was removed under vacuum. The solid was washed with pentane and crystallized from acetone (74% yield). Anal. Calcd for $\text{C}_{36}\text{H}_{44}\text{F}_6\text{CuP}_2\text{Ta}$: C, 48.2; H, 5.0. Found: C, 49.1; H, 4.8.

[(C₅H₄Bu^t)₂TaH₃Au(PPh₃)] [PF₆] was similarly prepared with $[\text{AuPPh}_3][\text{PF}_6]$ (82% yield). Anal. Calcd for $\text{C}_{36}\text{H}_{44}\text{F}_6\text{AuP}_2\text{Ta}$: C, 42.0; H, 4.3. Found: C, 41.3; H, 4.2.

Results and Discussion

Bimetallic complexes **1** and **2** are prepared from the trihydride $\text{Cp}'_2\text{TaH}_3$ according to the high-yield reaction of eq 1 where M



= Au (**1**) and Cu (**2**). The complexes are characterized by correct elemental analyses, and their structures are assigned spectroscopically (see the IR data in the Experimental Section and below) since it was not possible to grow crystals suitable for an X-ray analysis.

The room-temperature $^31\text{P}\{^1\text{H}\}$ NMR spectrum of an acetone- d_6 solution of **1** shows two resonances at 54.8 (PPh₃) and -140.9 (PF₆), $J(\text{P}-\text{F}) = 700$ Hz) ppm. The hydride region of the ^1H NMR spectrum of this solution exhibits an $^1\text{H}-^{31}\text{P}$ coupled AX₂ pattern with the parameters in Table 1. The $J(\text{H}-\text{P})$ coupling constants disappear in the $^1\text{H}\{^{31}\text{P}\}$ experiments. Lowering the temperature leads to a splitting of the H^X peak of intensity 2 ($\delta = 0.131$ ppm) into two new lines of intensity 1 at 0.493 and -0.437 ppm with $J(\text{H}-\text{P}) < 5$ and 36.7 Hz, respectively (Figure 1). The H^A ligand now shows a resonance at -0.984 ppm with $J(\text{H}-\text{P}) = 63.8$ Hz. According to the data of Pignolet and co-workers,^{5a} the significant $J(\text{H}-\text{P})$ values, observed for two hydride lines at low temperatures, correspond to a structure with two bridging hydride ligands (Scheme 1). Very similar structures with two bridging hydrides were recently established for the bimetallic Nb complexes $[\{\text{Nb}(\text{C}_5\text{H}_3\text{RR}')_2\text{H}_3\}_2\text{M}]$ with M = Cu, Ag, and Au^{5b} and for $[\{\text{Ru}(\text{C}_5\text{H}_5)\text{H}_3(\text{PCy}_3)_2\}_2\text{M}]$ (M

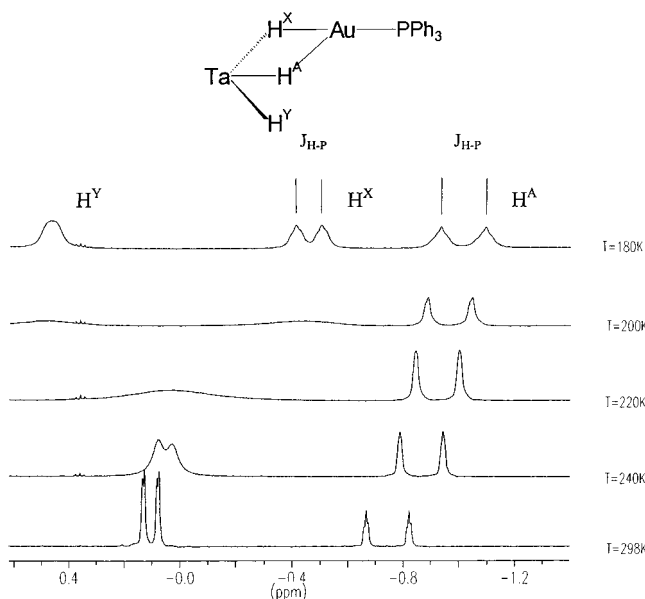
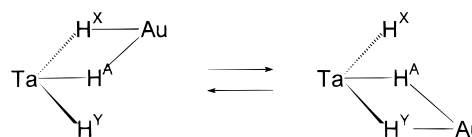


Figure 1. Hydride region in the variable-temperature ^1H NMR spectra of an acetone- d_6 solution of tantalum-gold complex **1** at 400 MHz.

Scheme 1



= Cu, Ag, and Au),^{5c} where the phosphorus ligand is bound to the Ru atom. It is interesting that the low-temperature ^1H NMR spectra of the complex $[\{\text{Ru}(\text{C}_5\text{H}_5)\text{H}_3(\text{PCy}_3)_2\}_2\text{Cu}]$ showed a coupling to ^{31}P only for the terminal hydride ligand (25 Hz). The absence of the resolved $J(\text{H}-\text{P})$ constants for the bridging hydrides was explained by the authors in terms of a lengthening of the corresponding Ru-H distances.^{5c} The same approach can be used for complex **1**, where the phosphorus group is bound to the Au atom. Actually here the $J(\text{H}-\text{P})$ couplings are observed only for the bridging hydrides. These $J(\text{H}-\text{P})$ values indicate that Au is bound relatively strongly to the central hydride ligand and more weakly to the second bridging hydride.

The variable-temperature ^1H NMR spectra of **1** in Figure 1 demonstrate a fluxional process reflecting an intramolecular exchange between two outer hydride ligands (H^X and H^Y in Scheme 1). When the exchange is frozen on the NMR time scale, the signals of the Cp' rings also split, transforming to the lines at 5.526 and 5.434 ppm for Cp(H^a) and 6.091 and 6.044 ppm for Cp(H^b). The coalescence of resonances of the outer hydride ligands is observed at 210 K. Note that the ΔG^\ddagger value of 9.3 kcal/mol determined under these conditions is very close to that reported for $[\{\text{Nb}(\text{C}_5\text{H}_3\text{RR}')_2\text{H}_3\}_2\text{Au}]$ ^{5b} despite the presence of the donor PPh₃ ligand in complex **1**.

Complex **1** shows practically identical NMR parameters in acetone- d_6 , CDCl₃, and CD₂Cl₂. However, in DMSO (295 K), the hydride ligands are observed as a broadened *singlet* at -0.047 ppm and a very broadened doublet line at -0.934 ppm.

(4) (a) Leblanc, J. C.; Reynoud, J. F.; Moise, C. C. *R. Seances Acad. Sci., Ser. 2* **1982**, 295, 755. (b) Lippard, S. J.; Ucko, D. A. *Inorg. Chem.* **1968**, 7, 1051. (c) Know, S. A. R.; Stone, F. G. A. *J. Chem. Soc. A* **1969**, 2559.

(5) (a) Mueting, A. M.; Bos, W.; Alexander, B. D.; Boyle, P. D.; Casalnovi, J. A.; Balaban, S.; Ito, L. N.; Jonson, S. M.; Pignolet, L. H. *New J. Chem.* **1988**, 12, 505. (b) Antinolo, A.; Carrillo-Hermosilla, F.; Chaudret, B.; Fajardo, M.; Fernandez-Baeza, J.; Lanfranchi, M.; Limbach, H.-H.; Maurer, M.; Otero, A.; Pellinghelli, M. A. *Inorg. Chem.* **1996**, 35, 7873. (c) Manzano, B.; Matthes, J.; Sabo-Etienne, S.; Chaudret, B.; Ulrich, S.; Limbach, H.-H. *J. Chem. Soc., Dalton Trans.* **1997**, 3153.

Increasing the concentration of the solution or the temperature led to full loss of the $J(\text{H}-\text{P})$ splitting for the both hydride signals. Hence an *intermolecular* $\text{PPh}_3/\text{PPh}_3$ exchange operates on the NMR time scale in the more polar DMSO.

The room-temperature $^{31}\text{P}\{^1\text{H}\}$ NMR spectrum of bimetallic trihydride **2** (acetone- d_6) exhibits two lines at -4.3 (PPh_3) and -145.0 ($[\text{PF}_6]^-$, $J(\text{P}-\text{F}) = 700$ Hz) ppm. However, visible $J(\text{H}-\text{P})$ constants are absent in the ^1H NMR spectrum of **2** and the hydride ligands show a simple AX_2 pattern: $\delta(\text{H}^{\text{X}}) = -2.490$ ppm, $\delta(\text{H}^{\text{A}}) = -3.629$ ppm with $J(\text{H}^{\text{X}}-\text{H}^{\text{A}}) = 7.6$ Hz. It is obvious that the intermolecular $\text{PPh}_3/\text{PPh}_3$ exchange in **2** is significantly faster than that in **1**. It is interesting that both hydride lines of **2** are remarkably broadened and this effect increases with the temperature. We have found no saturation transfers for the hydride resonances even at 310 K (which could correspond to an exchange between H^{A} and H^{X}), and thus the broadening effects can be explained in terms of scalar relaxation of the second kind by coupling between ^1H and the quadrupolar Cu nuclei.⁶

As in the case of **1**, lowering the temperature of an acetone- d_6 solution of **2** yields a splitting of the H^{X} peak ($\delta = -2.490$ ppm) into two new lines with $\delta = -0.887$ and -4.351 ppm (190 K, 200 MHz). The full analysis of the line shapes between 190 and 280 K provided calculation of kinetic parameters for the exchange between two outer hydride ligands: $\Delta H^\ddagger = 8.6 \pm 0.2$ kcal/mol, $\Delta S^\ddagger = -5.0 \pm 0.4$ eu, and $\Delta G^\ddagger = 9.6 \pm 0.2$ kcal/mol (210 K). In agreement with the intramolecular character of the hydride exchange, the entropy is close to 0 eu. It is remarkable that, even at 190 K, the hydrides in **2** do not show the $J(\text{H}-\text{P})$ constants and thus the $\text{PPh}_3/\text{PPh}_3$ exchange remains fast on the NMR time scale. However this process was frozen in a weakly concentrated CD_2Cl_2 solution at 180 K (400 MHz). Under these conditions, the ^1H NMR spectrum exhibited three very broadened hydride lines at -1.058 , -4.208 , and -4.786 ppm, one of which (H^{A} , -4.208 ppm) showed a $J(\text{H}-\text{P})$ splitting of ~ 15 Hz. Note that increasing the temperature (283 K) leads to disappearance of this constant and observation of an AX_2 pattern with $\delta(\text{H}^{\text{X}}) = -2.680$ ppm, $\delta(\text{H}^{\text{A}}) = -3.830$ ppm, and $J(\text{H}^{\text{X}}-\text{H}^{\text{A}}) = 7.0$ Hz. Thus all the above spectral data allow us to formulate for **2** the hydride arrangement represented in Scheme 1.

The variable-temperature ^1H NMR data demonstrate the higher hydride fluxionality in the tantalum–gold compound. The same tendency was found for $[\{\text{Nb}(\text{C}_5\text{H}_3\text{RR}')_2\text{H}_3\}_2\text{M}]$ ($\text{M} = \text{Cu}, \text{Au}$) and discussed in terms of a less extended electronic cloud of ion Cu^+ which is more acidic and therefore more strongly bound to the hydrides.^{5b} We believe that the faster intermolecular $\text{PPh}_3/\text{PPh}_3$ exchange observed in **2** supports well this idea. It should be emphasized the exchanges between two outer hydrides in **1**, **2**, $[\{\text{Nb}(\text{C}_5\text{H}_3\text{RR}')_2\text{H}_3\}_2\text{M}]$ ($\text{M} = \text{Cu}, \text{Au}$),^{5b} and $[\{\text{Ru}(\text{C}_5\text{H}_5)\text{H}_3(\text{PCy}_3)_2\text{M}\}]$ ($\text{M} = \text{Cu}, \text{Au}$)^{5c} are characterized by similar activation parameters which are always higher for Cu. At the same time, the exchange between the central and outer hydride ligands is strongly dependent on the nature of the complexes. For example, in $[\{\text{Ru}(\text{C}_5\text{H}_5)\text{H}_3(\text{PCy}_3)_2\text{M}\}]$ ($\text{M} = \text{Cu}, \text{Au}$), this exchange is fast on the NMR time scale already at 280 K.^{5c} In **1**, **2**, and $[\{\text{Nb}(\text{C}_5\text{H}_3\text{RR}')_2\text{H}_3\}_2\text{M}]$,^{5b} the exchange remains very slow even at 310 K. These data support well the idea that the exchange between two outer hydrides is a coinage-metal transfer between the hydride sites.^{5c}

The AX_2 hydride spin system of tantalum–gold complex **1** shows an interesting feature: the $J(\text{H}^{\text{A}}-\text{H}^{\text{X}})$ value of 2.8 Hz

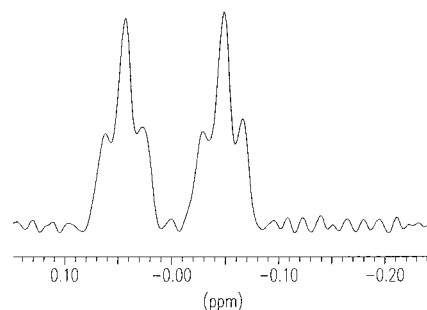
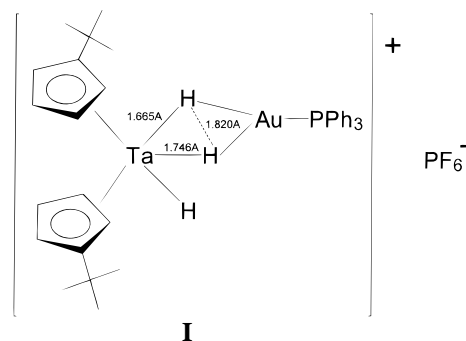


Figure 2. H^{X} resonance in the ^1H NMR spectrum of an acetone- d_6 solution of **1** at 180 K and 400 MHz.

(295 K, acetone- d_6) is significantly less than those for mononuclear Ta trihydrides,^{5b} their bimetallic derivatives $\text{Cp}_2\text{TaH}_2(\mu\text{H})\text{M}(\text{CO})_5$ ($\text{M} = \text{Cr}, \text{Mo}, \text{W}$) ($J(\text{H}-\text{H}) = 7.5-10.4$ Hz),⁷ and Cu complex **2** (7.8 Hz). This value slightly increases at 310 K (3.1 Hz). A similar unpronounced effect is also detected in a CDCl_3 solution of **1**: 2.5 and 3.6 Hz at 295 and 320 K, respectively. However when the exchange between two outer hydrides is frozen at 180 K (acetone- d_6 , 400 MHz) and the ^1H NMR spectrum of **1** contains three hydride lines (H^{A} , H^{X} , and H^{Y} ; for notation, see in Scheme 1), the H^{X} resonance clearly shows a triplet proton–proton splitting of 7.6 Hz (Figure 2). This constant is close to 7.8 and 8.8 Hz observed for tantalum–copper complex **2** and $[(\text{C}_5\text{H}_4\text{Si}(\text{CH}_3)_3)_2\text{TaH}_3]$,^{5b} respectively, and it can be attributed to a magnetic proton–proton coupling. Then the room-temperature $J(\text{H}^{\text{X}}-\text{H}^{\text{A}})$ value of 2.8 Hz for **1** can be explained by the presence of weak exchange $\text{H}^{\text{X}}-\text{H}^{\text{A}}$ couplings which are opposite in sign.⁸ Note that this conclusion is in good agreement with the data obtained for $[\{\text{Nb}(\text{C}_5\text{H}_3\text{RR}')_2\text{H}_3\}_2\text{M}]$ ^{5b} and $[\{\text{Ru}(\text{C}_5\text{H}_5)\text{H}_3(\text{PCy}_3)_2\text{M}\}]$,^{5c} where exchange couplings increase from Cu^+ to Au^+ .

The mutual orientation of the Cp' rings in **1** was determined by room-temperature NOE experiments in acetone- d_6 . CH_3 irradiation resulted in the positive NOE enhancement ($f = 0.1$) for one of the $\text{Cp}'(\text{H})$ lines with $\delta = 5.369$ ppm providing correct spectral assignments in Table 1. In accordance with these assignments, the $T_{1\text{min}}$ value of the $\text{Cp}(\text{H}^\alpha)$ protons is remarkably shorter (Table 1) due to dipole–dipole interactions with the CH_3 groups. Very weak NOE effects were observed for both $\text{Cp}'(\text{H})$ signals on H^{X} irradiation. Nevertheless the enhancement was more pronounced for the $\text{Cp}(\text{H}^\beta)$ resonance at 5.881 ppm. We believe that these results correspond to a maximally populated mutual arrangement of the Cp' rings represented in structure **I** where steric interactions between the trans-located bulky groups are minimal.



(6) Abragam, A. *The Principles of Nuclear Magnetism*; Oxford University Press; New York, 1971.

(7) Bakhtmutov, V. I.; Vorontsov, E. V.; Boni, G.; Moise, C. *Inorg. Chem.* **1997**, *36*, 4055.

(8) Heinekey, D. M. *J. Am. Chem. Soc.* **1991**, *113*, 6074.

Quantitative characterizations of the hydride arrangements in bimetallic complexes **1** and **2** can be carried out on the basis of ^1H T_1 relaxation data. Actually, in this case, only dipole–dipole proton–proton and proton–metal interactions dominate the hydride spin–lattice relaxation.^{3,9}

The total relaxation rate for the hydride ligands in **1** is described in terms of an isotropic model as follows:

$$1/T_1(\text{H}^{\text{A}}) = 1/T_1(\text{Ta}\cdots\text{H}^{\text{A}}) + 2/T_1(\text{H}^{\text{A}}\cdots\text{H}^{\text{X}}) + 1/T_1(\text{H}^{\text{A}}-\text{Cp}) + 1/T_1(\text{H}^{\text{A}}-\text{CH}_3) + 1/T_1(\text{H}^{\text{A}}-\text{Ph}) \quad (2\text{a})$$

$$1/T_1(\text{H}^{\text{X}}) = 1/T_1(\text{Ta}\cdots\text{H}^{\text{X}}) + 1/T_1(\text{H}^{\text{A}}\cdots\text{H}^{\text{X}}) + 1/T_1(\text{H}^{\text{X}}-\text{Cp}) + 1/T_1(\text{H}^{\text{X}}-\text{CH}_3) + 1/T_1(\text{H}^{\text{X}}-\text{Ph}) \quad (2\text{b})$$

In turn

$$1/T_1(\text{Ta}\cdots\text{H}) = 2\gamma_{\text{H}}^2\gamma_{\text{Ta}}^2h^2I(I+1)/15r_{\text{Ta}\cdots\text{H}}^6(3\tau_{\text{c}}/(1+\omega_{\text{H}}^2\tau_{\text{c}}^2) + 6\tau_{\text{c}}/(1+(\omega_{\text{H}}+\omega_{\text{Ta}})^2\tau_{\text{c}}^2) + \tau_{\text{c}}/(1+(\omega_{\text{H}}-\omega_{\text{Ta}})^2\tau_{\text{c}}^2)) \quad (3)$$

and

$$1/T_1(\text{H}\cdots\text{H}) = 0.3\gamma_{\text{H}}^4h^2/r_{\text{H}\cdots\text{H}}^6(\tau_{\text{c}}/(1+\omega_{\text{H}}^2\tau_{\text{c}}^2) + 4\tau_{\text{c}}/(1+4\omega_{\text{H}}^2\tau_{\text{c}}^2)) \quad (4)$$

where γ , h , I , and ω are well-known physical parameters and $\tau_{\text{c}} = \tau_0 \exp(E_{\text{a}}/RT)$.^{3,6,9} When the T_1 time in eq 3 or 4 reaches a minimum, the corresponding internuclear distances are calculated from eq 5 or 6 written in a convenient form (here ν is the ^1H NMR resonance frequency in MHz):

$$r_{\text{H}\cdots\text{H}} (\text{\AA}) = 2.405(200T_{1\text{min}}(\text{H}-\text{H})/\nu)^{1/6} \quad (5)$$

$$r_{\text{Ta}\cdots\text{H}} (\text{\AA}) = 2.001(200T_{1\text{min}}(\text{Ta}-\text{H})/\nu)^{1/6} \quad (6)$$

It is obvious that correct separations of the relaxation contributions in eqs 2 provide quantitative localization of the hydride ligands in the TaH_3 fragment. It should be emphasized that influence of ^{197}Au is negligible because of the small values of γ_{Au} and I_{Au} ($3/2$). Finally, it should be noted that the above equations are quite valid for isolated spins. In the case of AX_2 or more complicated spin systems, strong interpretation of their relaxation properties requires a Redfield density matrix treatment.¹⁰ However, this more correct (and more difficult) method is used for an opposite task—suggestion of a model of molecular motions in liquids on the basis of relaxation measurements and known geometrical data.¹⁰ In addition, note that the simple equations (2)–(6), even though not strictly correct, usually proved internuclear distances in good agreement with structural data.^{3c}

As predicted by the relaxation theory, the temperature T_1 dependencies give “V-shaped” plots (Figure 3 shows one of them) reaching minimum values at similar temperatures for all the protons of **1**. One can think that effects connected with *anisotropic molecular motions*¹⁰ of bimetallic complex **1** are not dramatic. In accordance with this conclusion, the $T_{1\text{min}}$ values measured at 400 MHz ($T_{1\text{min}}(\text{H}^{\text{X}}) = 0.180$ s, $T_{1\text{min}}(\text{H}^{\text{A}}) = 0.138$ s at 220 K) are close to those expected on the basis of the relaxation data collected at 200 MHz (Table 1). In addition,

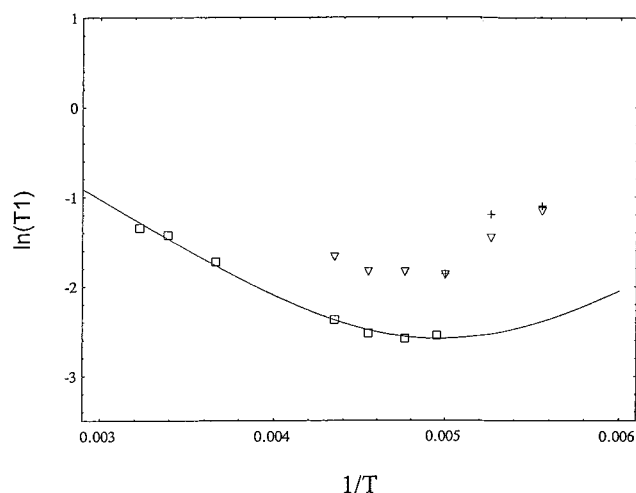


Figure 3. Variable-temperature T_1 dependencies for the hydride ligands in complex **1** (acetone- d_6): \square , H^{A} at 200 MHz; ∇ , H^{X} at 400 MHz; $+$, H^{Y} at 400 MHz (for notation, see in Scheme 1). The solid line corresponds to calculations.

Table 2. T_1 Data Collected for H^{X} of Complex **1** in Acetone- d_6 at 273 K and 200 MHz

parameter	value, s	parameter	value, s
T_1	0.280 (0.385) ^a	$T_{1\text{bis}}(\text{H}^{\text{X}}-\text{CH}^{\text{a}})$	0.365
$T_{1\text{sel}}$	0.380 (0.528) ^a	$T_{1\text{bis}}(\text{H}^{\text{X}}-\text{H}^{\text{A}})$	(0.442) ^a
$T_{1\text{bis}}(\text{H}^{\text{X}}-\text{CH}_3)$	0.344 (0.488) ^a	$T_{1\text{min}}$ (210 K)	0.0962
$T_{1\text{bis}}(\text{H}^{\text{X}}-\text{Ph})$	0.383	$T_{1\text{min}}(\text{H}^{\text{X}}-\text{H}^{\text{A}})$ (210 K)	0.185 ^b
$T_{1\text{bis}}(\text{H}^{\text{X}}-\text{CH}^{\text{b}})$	0.363	$T_{1\text{min}}(\text{H}^{\text{X}}-\text{Ta})$ (210 K)	0.292 ^b

^a At 295 K. ^b These values were calculated by averaging the $T_{1\text{sel}}/T_1$ ratios obtained in the relaxation experiments at different temperatures.

the calculation of the T_1 dependence in Figure 3 gives very reasonable E_{a} (2.6 kcal/mol) and τ_0 (5.6×10^{-13} s) values. Thus the T_1 data can be treated in terms of an isotropic model.

It follows from the relaxation experiments (Table 1) that the $T_{1\text{min}}$ times of the hydride ligands in Ta/Au complex **1** are remarkably shorter than those in mononuclear complex $[\text{C}_5\text{H}_4\text{Si}(\text{CH}_3)_3]_2\text{TaH}_2\text{H}^{\text{A}}$ (0.102 and 0.157 s for H^{A} and H^{X} , respectively, at 200 MHz^{5b}) or binuclear complexes $\text{Cp}_2\text{TaH}_2(\mu\text{-H})\text{M}(\text{CO})_5$ ($\text{M} = \text{Cr}, \text{Mo}, \text{W}$) containing one bridging hydride.⁷ Hence, the TaH_3 fragment undergoes remarkable structural changes when two hydride ligands are bound to the second metal center. At the same time, the $T_{1\text{min}}$ value for H^{X} in **1** is elongated with respect to 0.0696 s (200 MHz) measured in *cis*- $\{\text{Cp}_2\text{TaH}_2[\text{P}(\text{OMe})_3]\}$, where the hydride ligands are separated by only 1.67 \AA .¹¹

The variable-temperature T_1 experiments showed two distinct values for the H^{X} and H^{A} hydrides in **1**, demonstrating the lack of an $\text{H}^{\text{A}}/\text{H}^{\text{X}}$ exchange between 180 and 295 K. Hence the Ta–H bond lengths can be determined from measurements of selective ($T_{1\text{sel}}$), nonselective (T_1), and $T_{1\text{min}}$ relaxation times:³

$$r_{\text{Ta}\cdots\text{H}} = 3.736((1.4k + 4.47)T_{1\text{min}}/\nu)^{1/6} \quad (7)$$

In eq, 7 $k = (T_{1\text{sel}}/T_1 - 1)/(0.5 - T_{1\text{sel}}/3T_1)$ and the T_1 and $T_{1\text{sel}}$ times are measured at $\omega_{\text{H}}^2\tau_{\text{c}}^2 \ll 1$.^{3a}

The $T_{1\text{sel}}/T_1$ experiments (some of them are presented in Table 2) were carried out for H^{X} in acetone- d_6 between 273 and 295 K and in DMSO at 320 K. The determined $T_{1\text{sel}}/T_1$ ratios (eq 7) were averaged and used for further calculations of $r(\text{Ta}-\text{H}^{\text{X}})$

(9) Desrosiers, P. J.; Cai, L.; Lin, Z.; Richards, R.; Halpern, J. J. *Am. Chem. Soc.* **1991**, *113*, 4173.

(10) Grant, D. M.; Mayne, C. L.; Liu, F.; Xiang, T. X. *Chem. Rev.* **1991**, *91*, 1591 and references therein.

(11) Sabo-Etienne, S.; Chaudret, B.; Ulrich, S.; Limbach, H. H.; Moise, C. *J. Am. Chem. Soc.* **1995**, *117*, 11602.

(1.66 ± 0.03 Å). As mentioned above, the H^A line for **1** shows the large $J(H-P)$ constant of 62 Hz that strongly complicates $T_{1\text{sel}}$ measurements. The splitting disappears in DMSO at 320 K due to the fast intermolecular PPh_3/PPh_3 exchange, and this circumstance was used in order to measure the T_1 and $T_{1\text{sel}}$ times for H^A . These experiments led to determination of the corresponding Ta– H^A bond length (1.75 ± 0.03 Å).

Due to tantalum–hydride dipole–dipole interactions in eq 6, the obtained Ta– H^X and Ta– H^A distances provide 29% and 17% of the total relaxation rate: $1/T_{1\text{min}}(H^X)$ and $1/T_{1\text{min}}(H^A)$, respectively. To determine other relaxation contributions in eq 2, we have carried out the measurements of bisselective T_1 times for resonance pairs H^X/CH_3 , H^X/Ph , $H^X/Cp(H)$, and H^X/H^A (Table 2). Actually, magnitudes $F(H^X) = [1/T_{1\text{bis}}(H^X) - 1/T_{1\text{sel}}(H^X)]/[1/T_1(H^X) - 1/T_{1\text{sel}}(H^X)]$ reflect the fractional contributions to the total relaxation rate of proton H^X via dipolar interactions with the corresponding protons.¹²

The data in Table 2 show that, among different dipole–dipole proton–proton interactions, only the H^X-H^A and H^X-CH_3 contributions play a remarkable role in the H^X relaxation (here $T_{1\text{sel}} > T_{1\text{bis}} > T_1$; in the other cases, $T_{1\text{sel}} \approx T_{1\text{bis}}$). Determination of the corresponding $F(H^X)$ values as contributions to $T_{1\text{min}}(H^X)$ and calculation of $T_{1\text{min}}(\text{Ta}-H^X)$ from $r(\text{Ta}-H^X)$, obtained by the $T_{1\text{sel}}/T_1$ experiments, result in the contribution $1/T_{1\text{min}}(H^A \cdots H^X)$ reflecting the distance between H^A and H^X through eq 5.

The treatment of all the relaxation data gives the final localization of the hydride ligands in **1**: $r(\text{Ta}-H^X) = 1.66 \pm 0.03$ Å, $r(\text{Ta}-H^A) = 1.75 \pm 0.03$ Å, and $r(H^X \cdots H^A) = 1.82 \pm 0.03$ Å (structure **1**). These distances seem to be slightly shorter than those in the trihydride Cp_2TaH_3 determined by neutron diffraction: $r(\text{Ta}-H) = 1.774(3)$ Å and $r(H \cdots H) = 1.851$ Å.¹³ Nevertheless, they reproduce well the tendencies observed in the high-quality X-ray structure of $[\{Nb(C_5H_3RR')_2H_3\}_2Au][PF_6]$ ($R = R' = Si(CH_3)_3$) with two bridging hydrides.^{5b} Here the corresponding Nb– H^X , Nb– H^A , and $H^X \cdots H^A$ distances are found as 1.77(10), 1.94(10), and 2.12(14) Å, respectively.

(12) Siguira, M.; Takao, N.; Fujiwara, H. *Magn. Reson. Chem.* **1988**, *26*, 1051.

(13) Wilson, R. D.; Koetzle, T. E.; Hart, D. W.; Kvick, A.; Tipton, D. L.; Bau, R. *J. Am. Chem. Soc.* **1977**, *99*, 1775.

Finally, it should be emphasized that the exchange between two outer hydrides in **1** becomes slow below the $T_{1\text{min}}$ temperature, and therefore it was not possible to measure a relaxation difference for the bridging H^X and terminal H^Y ligands. It is probable that this exchange slightly distorts the found Ta–H and $H \cdots H$ distances.

The relaxation times of all the protons in **1** and **2** (acetone- d_6) pass through a minimum at similar temperatures (Table 1) that corresponds well to similar inertia moments of these molecules. The $T_{1\text{min}}$ values of the hydride ligands in **1** and **2** are practically identical, reflecting similar hydride arrangements in both compounds. Some decrease of the $T_{1\text{min}}$ values for the hydride ligands in **2** could be explained by the presence of ^{63}Cu ($I = 3/2$) and ^{65}Cu ($I = 3/2$).

Conclusions

The detailed NMR study of tantalum–gold and tantalum–copper trihydrides **1** and **2** has demonstrated how $T_{1\text{min}}$, T_1 , $T_{1\text{sel}}$ and $T_{1\text{bis}}$ measurements can be used for quantitative localization of the hydride ligands in solutions of bimetallic complexes. The determined hydride–hydride and metal–hydride distances reproduce well the structural tendencies in the related niobium trihydride $[\{Nb(C_5H_3RR')_2H_3\}_2Au][PF_6]$ ($R = R' = Si(CH_3)_3$) found by the X-ray method. The correct experimental estimations have demonstrated Ta–H dipole–dipole interactions to be important for the hydride relaxation in **1** providing 29% and 17% of the relaxation rate for H^X and H^A , respectively.

In good agreement with the literature data, complexes **1** and **2** contain two bridging Ta hydride ligands binding to the second metal center. The variable-temperature NMR data showed the fluxionality of both compounds. The intramolecular exchange between two outer hydride ligands is faster in **1** ($\Delta G^\ddagger = 9.3$ kcal/mol; 210 K) than in **2** ($\Delta H^\ddagger = 8.6 \pm 0.2$ kcal/mol, $\Delta S^\ddagger = -5.0 \pm 0.4$ eu, $\Delta G^\ddagger = 9.6 \pm 0.2$ kcal/mol; 210K). In contrast, complex **2** undergoes the faster intermolecular PPh_3/PPh_3 exchange.

The presented data can be considered as a development of the T_1 approaches for quantitative structural characterizations of metal–hydride moieties in solution.

IC980765W